

Supplementary Information

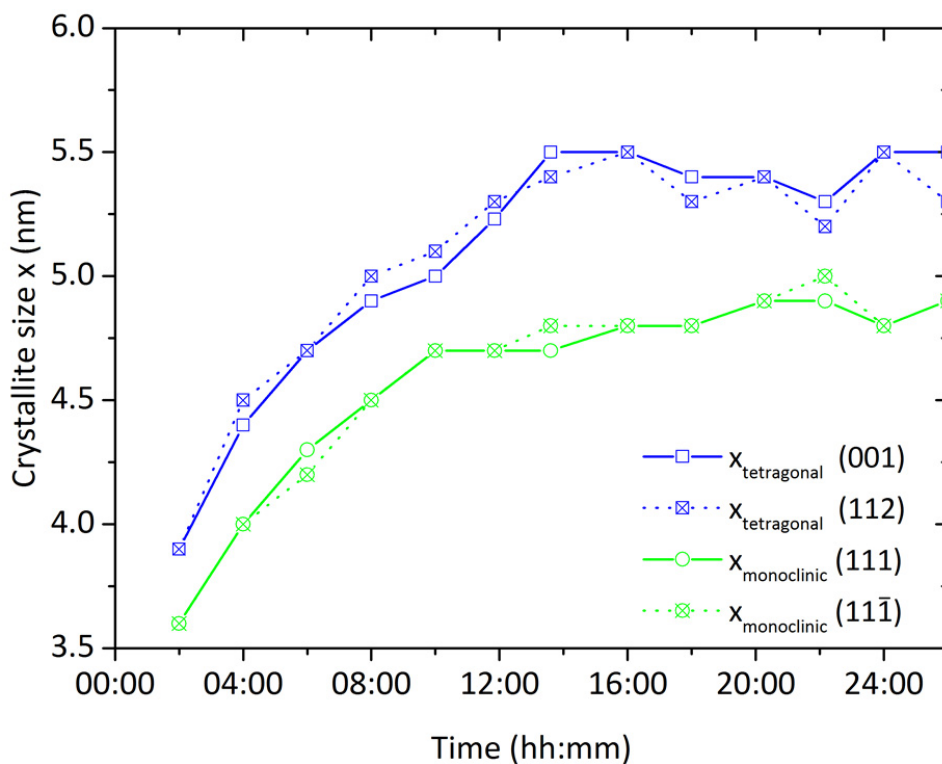


Fig. S. 1 Evolution of the crystal sizes determined by Rietveld refinement from the respective (001) and (112) lattice planes for the tetragonal polymorph (ICSD code: 98-006-6789) and the (111) and (11 $\bar{1}$) lattice planes of the monoclinic polymorph (ICSD code: 98-008-0045)

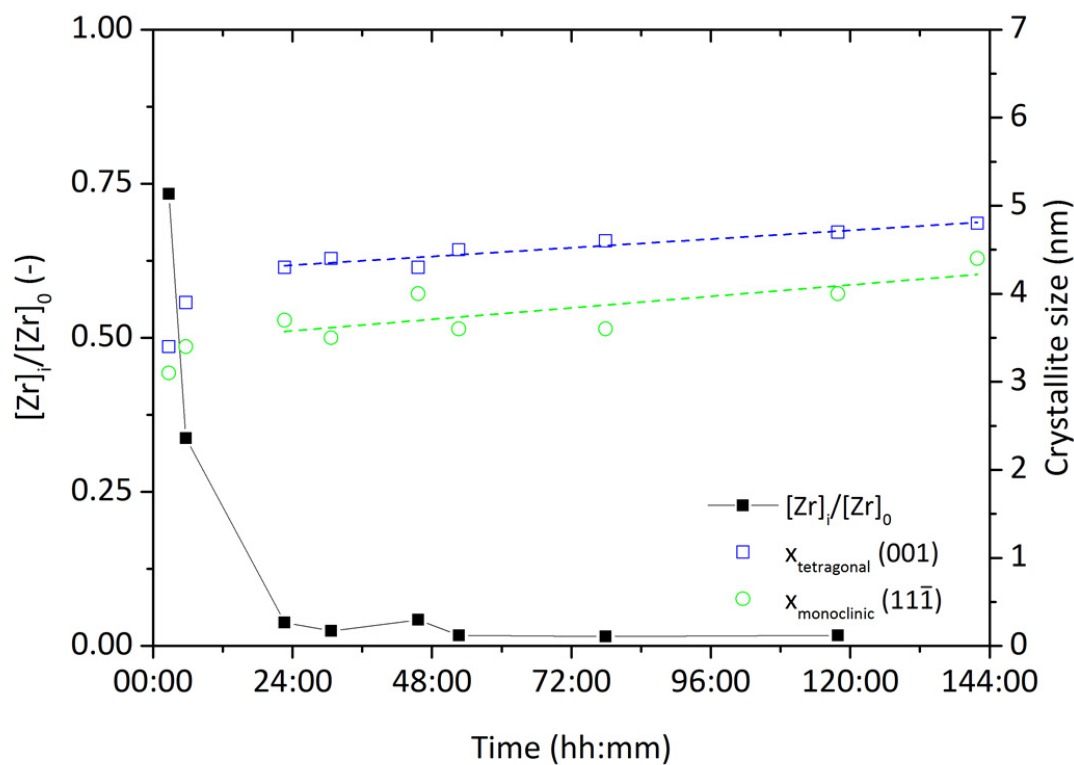


Fig. S. 2 Ostwald ripening during a standard synthesis ($T = 250\text{ }^{\circ}\text{C}$, initial precursor concentration $[Zr]_0 = 180\text{ mmol L}^{-1}$)

Surface bound ligands

The emerging nanoparticles contain a significant amount of organics on their surface Fig. S. 3, even after multiple washing steps. Thermogravimetric analysis (Fig. S. 4) indicates that the amount of adsorbed organics decreases over time. As previously shown by our group,¹ these surface organics are mostly chemisorbed BnO- ligands originating from the molecular processes that lead to ZrO₂ nanoparticle formation - considering that the Zr-O-Zr network forms by the reaction between alkoxy species $Zr(\text{OnPr})_{4-x}(\text{OBn})_x$, a certain amount of ligand species will be still linked to the zirconium atoms on the crystal surface via Zr-O-Bn and Zr-O-nPr bridges. The declining surface to volume ratio (A/V) Fig. S. 5 of the particles reduces the available surface area, leading to a decrease in the relative mass of chemisorbed organics. The amount of physisorbed benzyl alcohol and other volatiles also decreases, but is according to TGA compared to the amount of chemisorbed ligands, such as benzoate or other organics,² smaller in quantity.

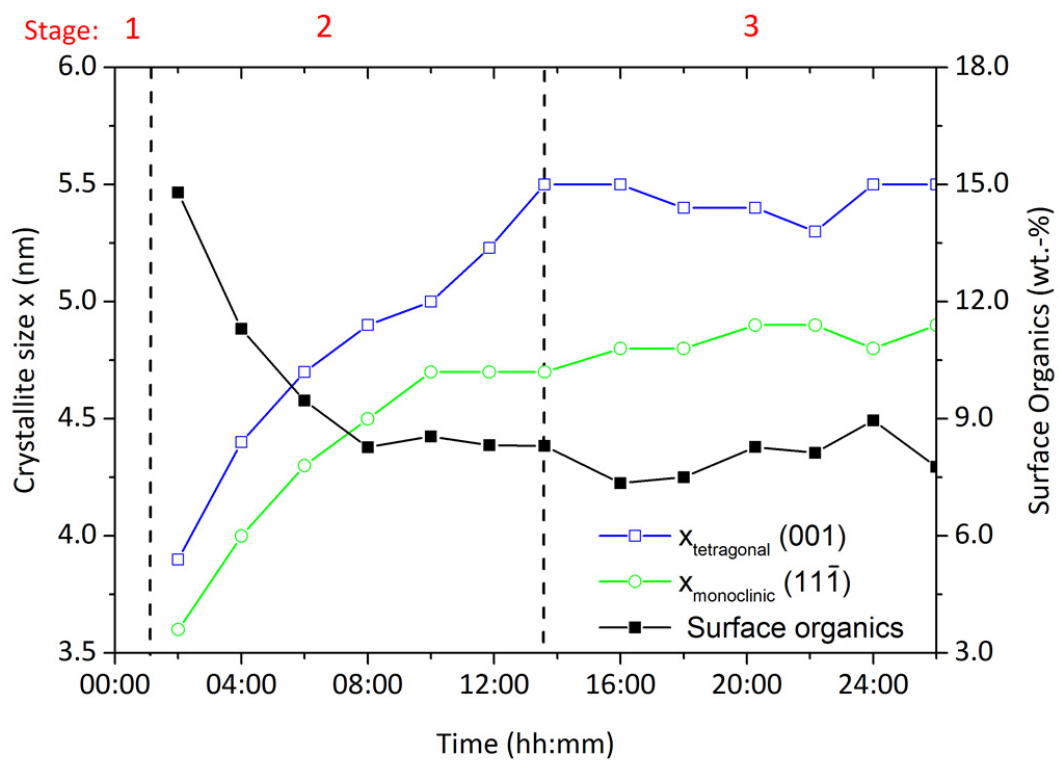


Fig. S. 3 Development of crystallite size and content of surface organics during a synthesis at 250 °C; Stage 1 heating period; Stage 2 particle formation; Stage 3 catalytic condensation reaction

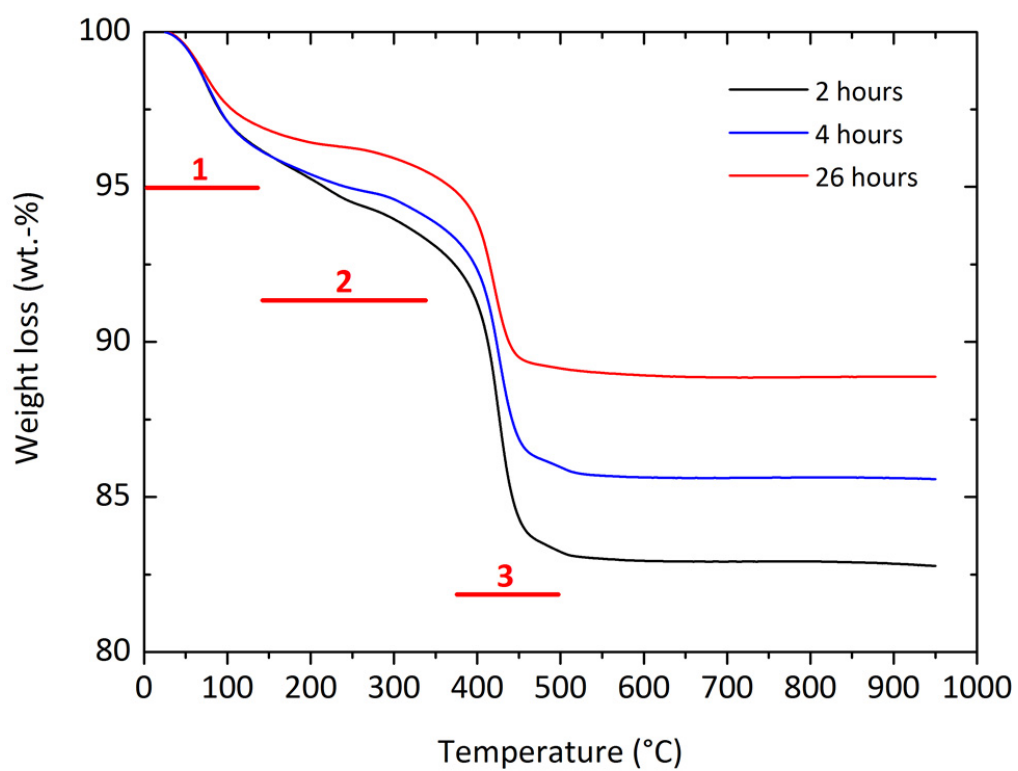


Fig. S. 4 Thermogravimetric analysis of samples during a standard synthesis; 1 weight loss due to dehydration and volatile organics, 2 weight loss due to physisorbed BnOH and chemisorbed benzoates, 3 weight loss due to decomposition of chemisorbed BnO⁻ ligands¹

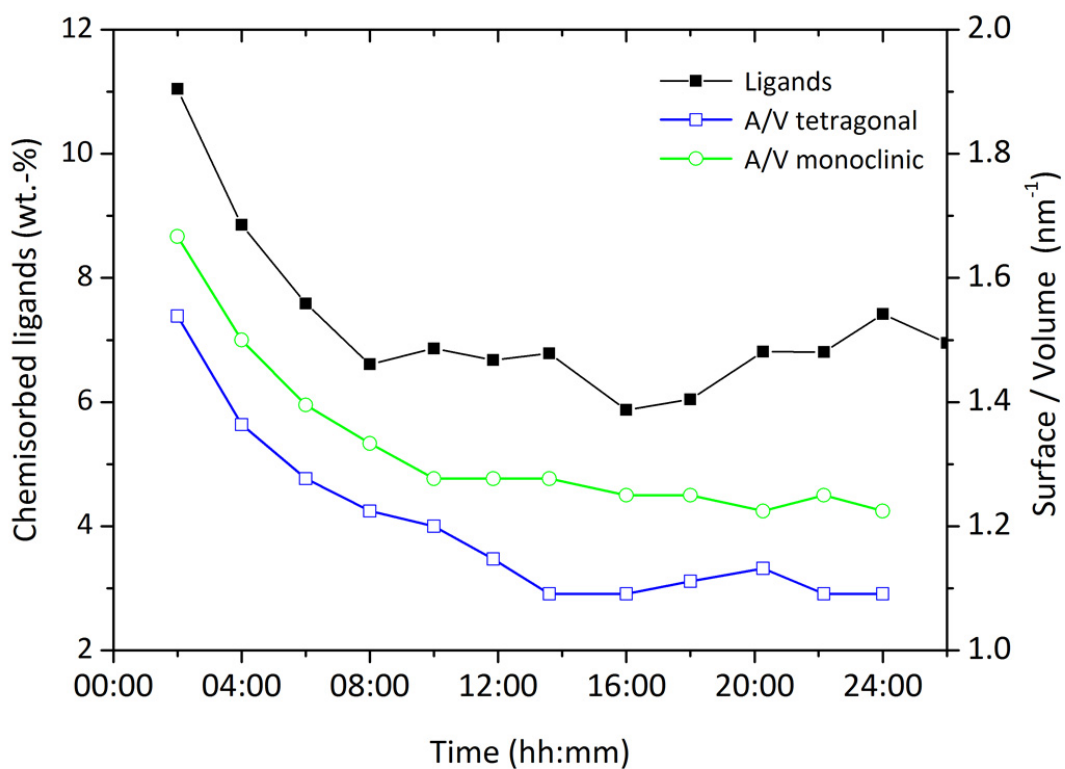


Fig. S. 5 Surface to Volume ration A/V and ligands over time for a standard synthesis

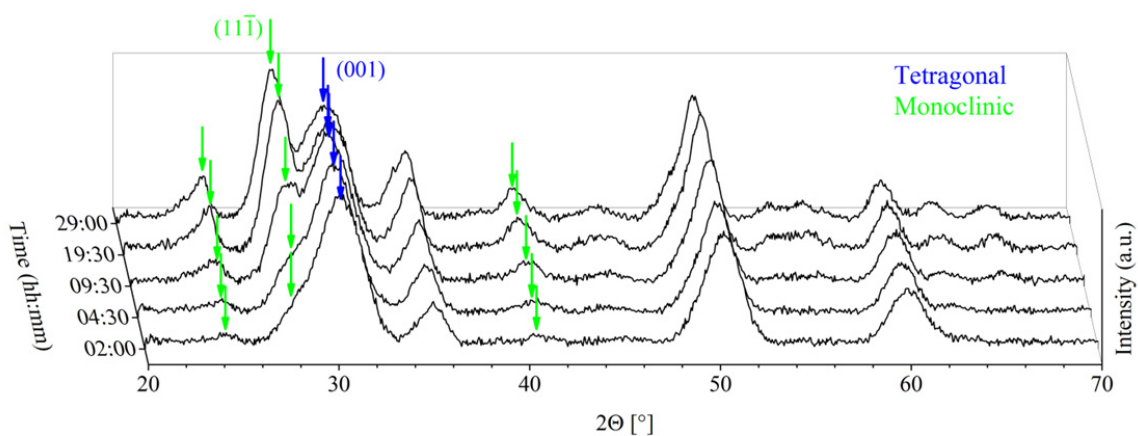


Fig. S. 6 XRD patterns during a synthesis at 240 °C and $[Zr]_0$ 180 mmol L⁻¹ undergoing a tetragonal to monoclinic phase transition

Table 1 Phase composition, crystallite sizes and specific surface area for the products obtained at different synthesis conditions

[Zr] ₀ (mmol L ⁻¹)	T (°C)	Tetragonal crystal size x _t (nm)	Monoclinic crystal size x _m (nm)	Monoclinic phase content (vol.-%)	Specific surface area (m ² g ⁻¹)
180	250	5.5	4.9	56.0	66.05
240	250	6.1	4.7	57.0	-
360	250	5.3	4.6	63.0	47.19
180*	250	3.9	3.1	22.2	-
180	220	4.9	4.3	59.6	116.05
240	220	4.9	4.4	61.2	-
360	220	6.0	5.9	81.5	-
180	230	5.7	4.6	74.6	72.32
360	230	5.6	4.2	75.3	-
180	240	6.1	4.7	82.0	107.23
180	270	3.6	2.7	18.2	13.41
240	270	3.9	2.5	26.0	-
360	270	3.7	4.6	22.0	-

* Seeded with 1 wt.-% final product suspension of a run performed at equal conditions

1. T. A. Cheema and G. Garnweitner, *CrystEngComm*, 2014, **16**, 3366-3375.
2. T. A. Cheema, Dissertation, Technische Universität Braunschweig, 2013.